Near field acoustic holography based on the equivalent source method and pressure-velocity transducers

Zhang, Y.-B.; Chen, X.-Z.; Jacobsen, Finn

Published in:
Acoustical Society of America. Journal

Link to article, DOI:
10.1121/1.3179665

Publication date:
2009

Document Version
Publisher's PDF, also known as Version of record

Near field acoustic holography based on the equivalent source method and pressure-velocity transducers

Yong-Bin Zhang[a)]
Institute of Sound and Vibration Research, Hefei University of Technology, Hefei 230009, China

Finn Jacobsen
Department of Electrical Engineering, Acoustic Technology, Technical University of Denmark, Building 352, Ørsteds Plads, DK-2800 Kongens, Lyngby, Denmark

Chuan-Xing Bi and Xin-Zhao Chen
Institute of Sound and Vibration Research, Hefei University of Technology, Hefei 230009, China

(Received 2 January 2009; revised 26 May 2009; accepted 18 June 2009)

The advantage of using the normal component of the particle velocity rather than the sound pressure in the hologram plane as the input of conventional spatial Fourier transform based near field acoustic holography (NAH) and also as the input of the statistically optimized variant of NAH has recently been demonstrated. This paper examines whether there might be a similar advantage in using the particle velocity as the input of NAH based on the equivalent source method (ESM). Error sensitivity considerations indicate that ESM-based NAH is less sensitive to measurement errors when it is based on particle velocity input data than when it is based on measurements of sound pressure data, and this is confirmed by a simulation study and by experimental results. A method that combines pressure- and particle velocity-based reconstructions in order to distinguish between contributions to the sound field generated by sources on the two sides of the hologram plane is also examined. © *2009 Acoustical Society of America.* [DOI: 10.1121/1.3179665]

PACS number(s): 43.60.Sx, 43.60.Pt, 43.20.Rz [EGW] Pages: 1257–1263

I. INTRODUCTION

Near field acoustic holography (NAH) is a powerful tool for visualizing sound fields radiated by complicated sound sources. In addition to the classical NAH technique based on spatial discrete Fourier transforms,[1–3] many alternative methods have been developed in the past years, e.g., the inverse boundary element method,[4–6] the statistically optimized method,[7,8] the Helmholtz equation least-squares method,[9,10] and the equivalent source method (ESM) (also known as the wave superposition method).[11–16] Usually the measured quantity is the sound pressure rather than the particle velocity, simply because pressure microphones are readily available and easy to calibrate whereas the particle velocity has been difficult to measure. However, in recent years, a particle velocity transducer called Microflown has appeared.[17] Conventional planar NAH based on measurement of particle velocity was first considered by Jacobsen and Liu.[18] As they demonstrated, NAH based on measurement of the particle velocity transducers performs very well compared with pressure-based NAH. Statistically optimized NAH based on measurement of particle velocity has also been investigated, and the results showed a similar advantage.[19] In addition, a so-called *p-u* method based on combined measurements of the pressure and the particle velocity was proposed. Measuring both quantities makes it possible to overcome the usual requirement of a source free region on the other side of the hologram plane.[19]

The purpose of this paper is to examine the performance of NAH based on the ESM and measurements with particle velocity transducers. The combination of the *p-u* method and NAH based on ESM is also examined.

II. OUTLINE OF THEORY

A. ESM based on measurement of sound pressure

ESM is based on the idea of modeling the sound field generated by a vibrating structure by a set of simple sources placed in the interior of the structure. Such a superposition has been proved to be mathematically equivalent to the Helmholtz integral formulation.[11] Given that M measurement points are selected on the hologram surface and the number of the equivalent sources is N, the pressure column vector $\mathbf{P}_h$ at the measurement positions can be represented in matrix form as

$$\mathbf{P}_h = i\rho ck\mathbf{G}_{hp}\mathbf{Q}, \tag{1}$$

where ρ is the density of the medium, c is the speed of sound, $k=\omega/c$ is the wave number, ω is the angular frequency, $\mathbf{Q}=[q(\mathbf{r}_{o1}),q(\mathbf{r}_{o2}),\ldots,q(\mathbf{r}_{oN})]^T$ is the column vector with the strengths of the equivalent sources $q(\mathbf{r}_{on})$, $\mathbf{r}_{on}$ is the location vector of the nth equivalent source, and $\mathbf{G}_{hp}$ is the complex transfer matrix obtained from Green's function,

$$\mathbf{G}_{hp}|_{m,n} = g(\mathbf{r}_{hm},\mathbf{r}_{on}) = -\frac{e^{ikr}}{4\pi r}, \quad r=|\mathbf{r}_{hm}-\mathbf{r}_{on}|, \tag{2}$$

in which $\mathbf{r}_{hm}$ is the location vectors of the mth measurement point and g is the free space Green's function with the $e^{-i\omega t}$

a)Author to whom correspondence should be addressed. Electronic mail: zybmy1997@163.com

sign convention. The unknown source strength vector $\mathbf{Q}$ can be obtained from the expression

$$\mathbf{Q} = \frac{1}{i\rho ck}\mathbf{G}_{hp}^{+}\mathbf{P}_h, \tag{3}$$

where the generalized inverse matrix $\mathbf{G}_{hp}^{+}$ is obtained from $\mathbf{G}_{hp}$ by singular value decomposition. Once the source strength vector has been determined, the pressure and the normal velocity on the surface of the acoustic source can be reconstructed as

$$\mathbf{P}_s = i\rho ck\mathbf{G}_{sp}\mathbf{Q}, \tag{4}$$

$$\mathbf{U}_{ns} = \mathbf{G}_{sv}\mathbf{Q}, \tag{5}$$

where $\mathbf{P}_s$ and $\mathbf{U}_{ns}$ are the reconstructed pressure and normal velocity vectors on the surface of the source, and $\mathbf{G}_{sp}$ and $\mathbf{G}_{sv}$ are complex transfer matrices,

$$\mathbf{G}_{sp}|_{m,n} = g(\mathbf{r}_{sm}, \mathbf{r}_{on}), \tag{6}$$

$$\mathbf{G}_{sv}|_{m,n} = \frac{\partial g(\mathbf{r}_{sm}, \mathbf{r}_{on})}{\partial \mathbf{n}_s}. \tag{7}$$

In these expressions $\mathbf{r}_{sm}$ is the location vector of the mth point on the surface of the source, and $\mathbf{n}_s$ is the outward normal of the source.

B. ESM based on measurement of particle velocity

It is a simple matter to modify the foregoing to ESM based on measurement of the particle velocity. If the particle velocity normal to the measurement surface is measured at M points, then Eq. (1) is replaced with

$$\mathbf{V}_{nh} = \mathbf{G}_{hv}\mathbf{Q}, \tag{8}$$

where $\mathbf{V}_{nh}$ is a column vector of normal components of the particle velocity at the measurement positions, and $\mathbf{G}_{hv}$ is a complex transfer matrix,

$$\mathbf{G}_{hv}|_{m,n} = \frac{\partial g(\mathbf{r}_{hm}, \mathbf{r}_{on})}{\partial \mathbf{n}_h}, \tag{9}$$

in which $\mathbf{n}_h$ is the outward normal of the hologram surface. Once $\mathbf{Q}$ has been determined the reconstruction can be realized by Eqs. (4) and (5).

C. ESM based on measurement of pressure and particle velocity

It is impossible to distinguish between sounds generated by sources on the two sides of the hologram plane only from measurement of pressure or particle velocity. A separation technique is needed as, e.g., the double layer method proposed by Bi *et al.*,[20] or the slightly different method based on measurement of pressure and a finite difference estimate of the particle velocity proposed by Bi and Chen.[21] Here the somewhat simpler idea proposed by Jacobsen and Jaud is introduced,[19] and a *p-u* method based on measurement of both the pressure and the normal component of the particle velocity is developed. From Eqs. (3)–(5) and (8), the reconstructed pressure and particle velocity can be expressed as follows:

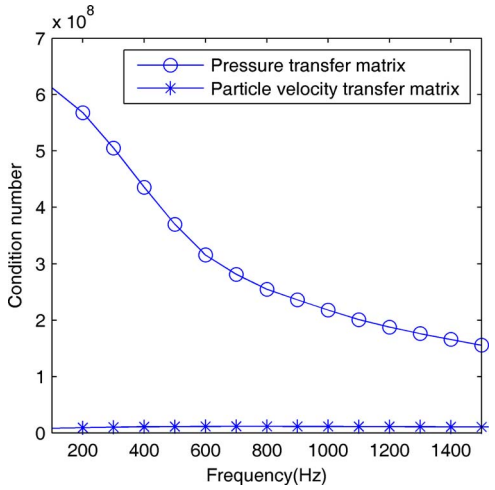

FIG. 1. (Color online) Condition number of transfer matrices.

$$\mathbf{P}_s = \frac{i\rho ck}{2}\mathbf{G}_{sp}\left(\frac{1}{i\rho ck}\mathbf{G}_{hp}^{+}\mathbf{P}_h + \mathbf{G}_{hv}^{+}\mathbf{V}_{nh}\right), \tag{10}$$

$$\mathbf{U}_{ns} = \frac{1}{2}\mathbf{G}_{sv}\left(\frac{1}{i\rho ck}\mathbf{G}_{hp}^{+}\mathbf{P}_h + \mathbf{G}_{hv}^{+}\mathbf{V}_{nh}\right). \tag{11}$$

The separation is possible because of the fact that the particle velocity is a vector component that changes sign, unlike the pressure, if the source is moved to a symmetrical position on the opposite side of the hologram plane. As in Ref. 19, one should perhaps not expect the same accuracy in the general case where the disturbing noise is not coming from a source placed symmetrically with respect to the hologram plane.

D. Error analysis and comparison of condition numbers

In practice, measured data are always contaminated by errors. Suppose that the real measured pressure and the normal component of the particle velocity can be written as follows:

$$\mathbf{P}_h = (\mathbf{P}_h)_r + (\mathbf{P}_h)_e, \tag{12}$$

$$\mathbf{V}_{nh} = (\mathbf{V}_{nh})_r + (\mathbf{V}_{nh})_e, \tag{13}$$

where the subscripts r and e denote the exact value and the error. Substituting Eqs. (12) and (13) into Eq. (5), the reconstructed surface normal velocity becomes

$$\mathbf{U}_{ns} = (\mathbf{U}_{ns})_r + (\mathbf{U}_{ns})_e = \frac{1}{i\rho ck}\mathbf{G}_{sv}\mathbf{G}_{hp}^{+}(\mathbf{P}_h)_r + \frac{1}{i\rho ck}\mathbf{G}_{sv}\mathbf{G}_{hp}^{+}(\mathbf{P}_h)_e \tag{14}$$

if it is based on pressure measurements, and

$$\mathbf{U}_{ns} = (\mathbf{U}_{ns})_r + (\mathbf{U}_{ns})_e = \mathbf{G}_{sv}\mathbf{G}_{hv}^{+}(\mathbf{V}_{nh})_r + \mathbf{G}_{sv}\mathbf{G}_{hv}^{+}(\mathbf{V}_{nh})_e \tag{15}$$

if it is based on velocity measurements. According to Ref. 16, an upper bound of the relative error of the reconstructed normal velocity can be expressed as

$$\frac{\|(\mathbf{U}_{ns})_e\|}{\|(\mathbf{U}_{ns})_r\|} \leq \begin{cases} \text{cond}(\mathbf{G}_{sv})\text{cond}(\mathbf{G}_{hp})\dfrac{\|(\mathbf{P}_h)_e\|}{\|(\mathbf{P}_h)_r\|} & \text{(pressure measurement)} \\ \text{cond}(\mathbf{G}_{sv})\text{cond}(\mathbf{G}_{hv})\dfrac{\|(\mathbf{V}_{nh})_e\|}{\|(\mathbf{V}_{nh})_r\|} & \text{(particle velocity measurement)}, \end{cases} \tag{16}$$

where $\|\cdot\|$ denotes the norm of a matrix, and cond $(\cdot)$ denotes the condition number of a matrix. Equation (16) demonstrates that the errors will be magnified by the condition number of the transfer matrix. It follows that if the two measurements have the same error level, the condition numbers of the transfer matrices $\mathbf{G}_{hp}$ and $\mathbf{G}_{hv}$ determine the influence of measurement error on the reconstructed velocity. A similar error expression can be obtained for the reconstructed pressure by replacing $\mathbf{G}_{sv}$ with $\mathbf{G}_{sp}$.

The condition number of $\mathbf{G}_{hv}$ is much smaller than the condition number of $\mathbf{G}_{hp}$ in near fields where NAH is used, which leads to the conclusion that NAH based on the particle velocity is less sensitive to measurement errors than pressure-based NAH. This is demonstrated by an example. Suppose that a planar acoustic source is located at $z=0$ with dimensions 0.6×0.6 m^2 and modeled with a grid of 21×21. The hologram plane and the equivalent source plane are located at $z=0.05$ m and $z=-0.03$ m, respectively, with the same dimension as the source and a grid of 31×31. The condition numbers of $\mathbf{G}_{hp}$ and $\mathbf{G}_{hv}$ are shown in Fig. 1. It is obvious that the condition number of $\mathbf{G}_{hv}$ is smaller than the condition number of $\mathbf{G}_{hp}$ in the entire frequency range from 100 to 1500 Hz. At low frequencies the condition number of $\mathbf{G}_{hp}$ is more than 70 times larger than that of $\mathbf{G}_{hv}$. The ratio decreases with the frequency but is still significant at the upper limiting frequency. Figure 2 shows all the singular values of $\mathbf{G}_{hp}$ and $\mathbf{G}_{hv}$ at 200 Hz. It can be seen that the singular values of $\mathbf{G}_{hp}$ decay faster than the singular values of $\mathbf{G}_{hv}$ (from similar high values), which explains why the pressure-based approach is more ill-posed than the particle velocity-based approach. Similar results have been obtained at other frequencies.

The condition number (the ratio of the largest to the smallest singular value) is a measure of the sensitivity of the solution of a system of linear equations to errors in the input data. If two columns of the corresponding matrix are nearly identical, the matrix is ill-conditioned, the condition number is large, and errors will be amplified. Thus the explanation for the observation that $\mathbf{G}_{hp}$ tends to be more ill-conditioned than $\mathbf{G}_{hv}$ is that the elements of the former are Green's function, whereas the elements of the latter are the *derivative* of Green's function. The derivative is much more sensitive to small changes in the argument of the function, $|\mathbf{r}_{hm}-\mathbf{r}_{on}|$, in agreement with the fact that whereas the pressure is inversely proportional to the distance to a monopole, the particle velocity is inversely proportional to the square of the distance very near the source.

In order to reduce the influence of the measurement errors, Tikhonov regularization is used to stabilize the computational process; and the regularization parameter is chosen by the L-curve method.[22]

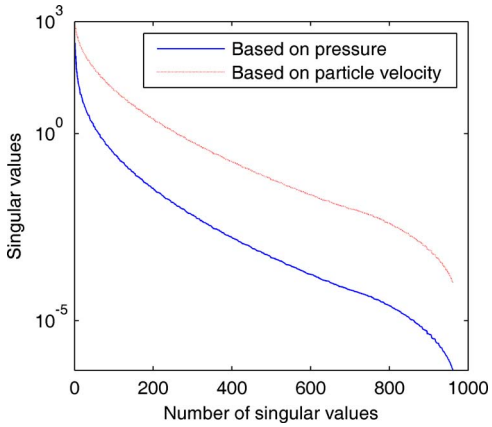

FIG. 2. (Color online) Singular values of the transfer matrices at 200 Hz.

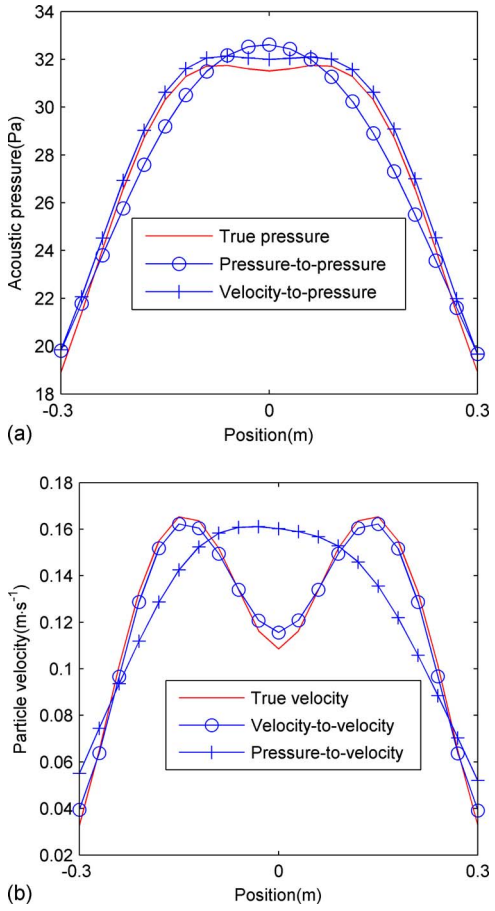

FIG. 3. (Color online) True and predicted pressure (a) and particle velocity (b) in the reconstruction plane, generated by a baffled vibrating panel at 100 Hz.

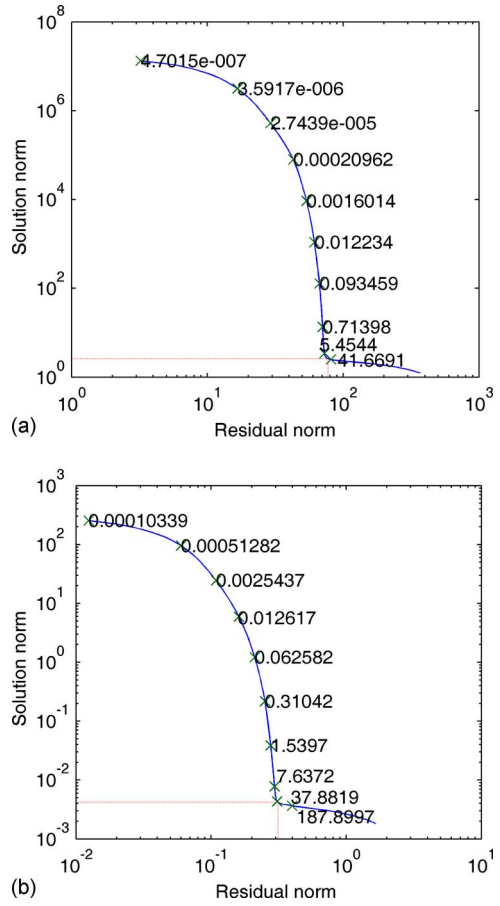

FIG. 4. (Color online) L-curves for determination of regularization parameter based on pressure (a) and on particle velocity (b). The position of the selected parameter is marked by dotted lines.

III. A SIMULATION STUDY

The condition number ratio found in the foregoing seems to indicate that it should be advantageous to measure the normal component of the particle velocity rather than the pressure in the hologram plane. To examine the matter a simulation study has been carried out. The test case was a point driven simply supported 3-mm-thick aluminum plate mounted in an infinite baffle. The dimensions, grid, and positions of the vibrating plate, the hologram plane, and the equivalent source plane were all the same as in the example presented above. The excitation of the plate was a harmonic force with an amplitude of 100 N acting at the center of the plate. The displacement and the normal velocity on the surface of the plate were calculated by modal superposition, and the radiated sound field was calculated from a numerical approximation to Rayleigh's first integral.[23] The reconstructed plane was located at $z=0.03$ m. In what follows, the "true" data have been calculated from the numerical approximation to Rayleigh's integral, and the reconstructed values have been calculated from the "measured" pressure or particle velocity.

A. ESM based on measurement of pressure or particle velocity

Figure 3(a) compares the true pressure along the x-axis at 100 Hz with reconstructions based on the pressure and

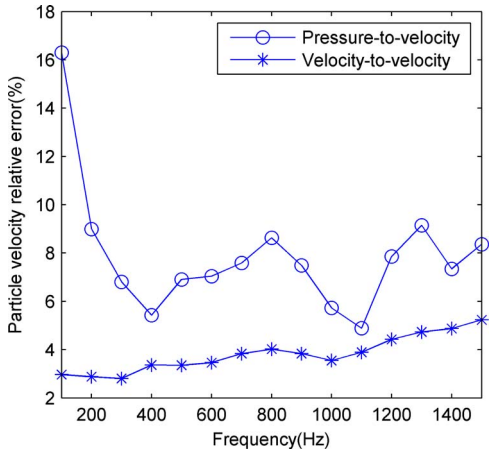

FIG. 5. (Color online) Relative error of reconstructed particle velocity.

based on the normal component of the particle velocity. To make the simulation study more realistic noise has been added to the measured data corresponding to a signal-to-noise ratio of 20 dB. It can be seen that the pressure reconstructed from velocity data is in better agreement with the true pressure than the pressure reconstructed from pressure data, which demonstrates that the method is less sensitive to

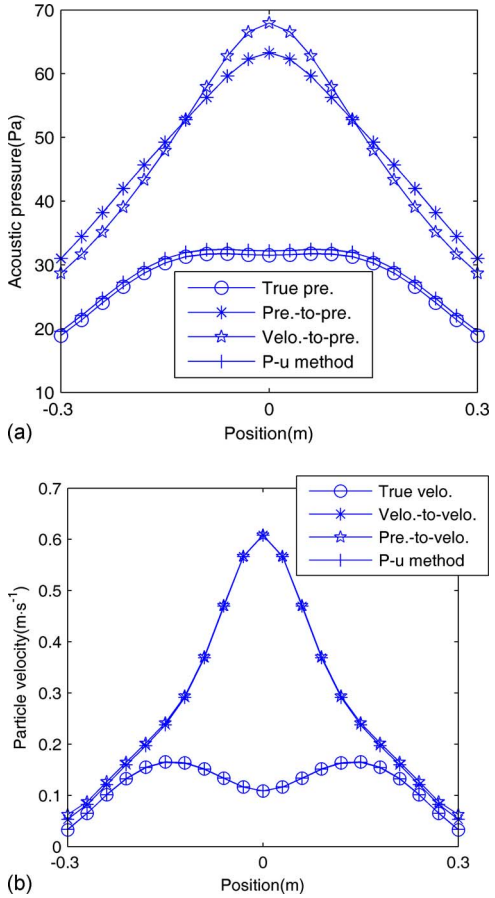

FIG. 6. (Color online) True and predicted undisturbed pressure (a) and particle velocity (b) in the reconstruction plane at 100 Hz. The primary source is a vibrating panel in a baffle, and the disturbing source is a monopole.

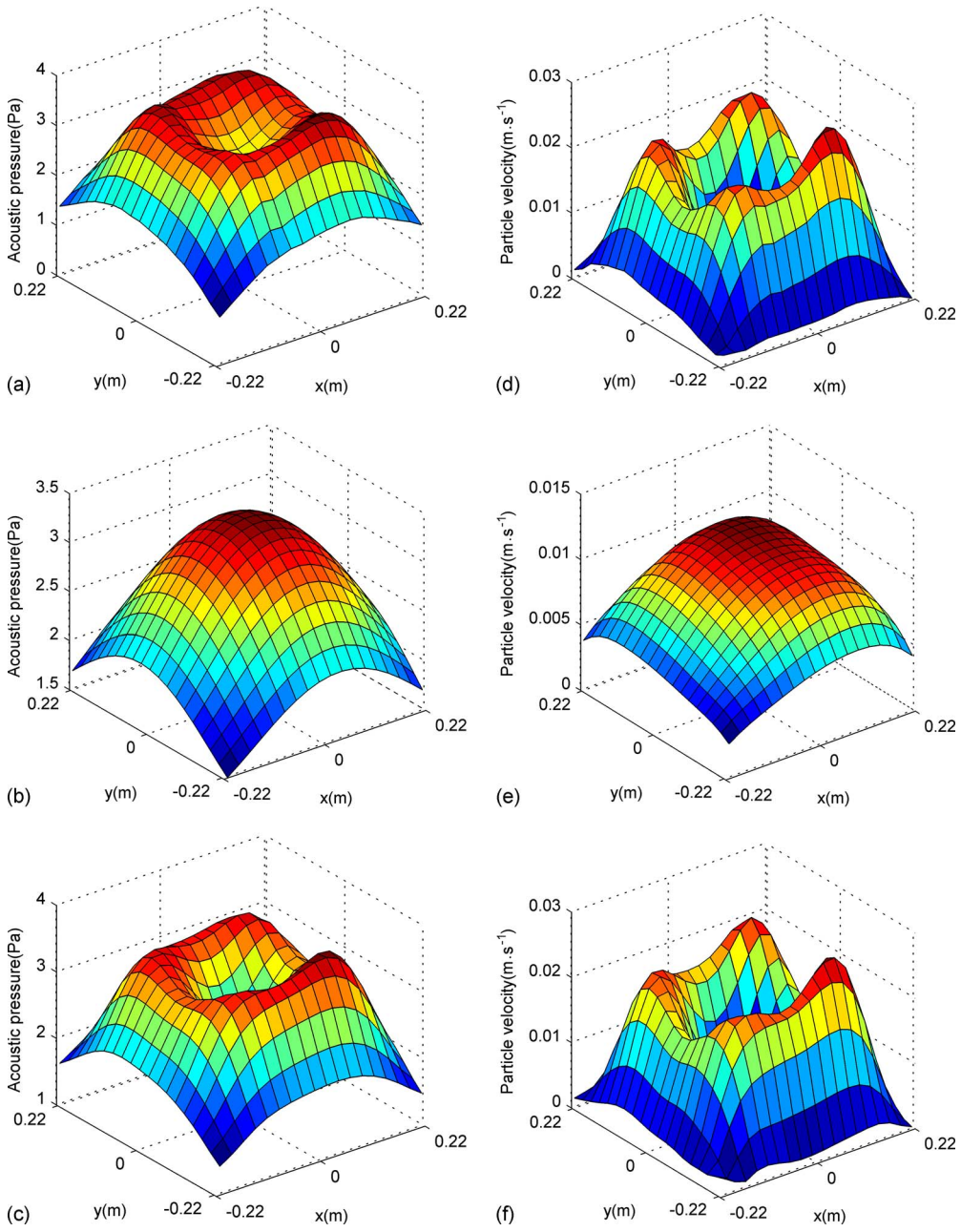

FIG. 7. (Color online) Sound field generated by a vibrating panel at 160 Hz. True pressure (a) and pressure predicted from pressure (b) and from particle velocity (c), and true particle velocity (d) and particle velocity predicted from pressure (e) and from particle velocity (f).

measurement errors if it is based on velocity data. This tendency is demonstrated even more clearly in Fig. 3(b), in which the true velocity and reconstructions based on the pressure and on the normal component of the particle velocity are compared; the reconstruction based on the particle velocity is by far the best. The L-curves for this case are shown in Fig. 4. The regularization parameters based on the pressure and on the velocity are both chosen reasonably near the corner of the curves. Similar results (not shown) have been found at other frequencies. Figure 5 shows the relative error as a function of the frequency. This quantity is defined as

$$\eta = \left(\sqrt{\sum_{i=1}^{N} |v_i - \hat{v}_i|^2} \Big/ \sqrt{\sum_{i=1}^{N} |v_i|^2} \right) \times 100\%, \qquad (17)$$

where N is the number of points on the reconstructed plane, and v_i and $\hat{v}_i$ are true and reconstructed normal velocities of the ith point. It is apparent that velocity-to-velocity results are better than pressure-to-velocity results in the entire frequency range, although the difference decreases with the frequency in agreement with the error analysis presented above.

B. ESM based on the *p-u* method

The *p-u* method is examined with a sound field generated by the same plate as described above and a monopole located at (0, 0, 0.2) (coordinates in meter), that is, on the other side of the hologram plane. (Reflections in the baffled panel have been ignored.) The disturbing source generates a higher pressure and a larger particle velocity than the primary source, the difference being up to 40%. The corresponding reconstructions in the prediction plane are shown in Figs. 6(a) and 6(b), which demonstrate that reconstructions based only on pressure or particle velocity are completely wrong, whereas the *p-u* method successfully separates the sound fields and gives results in good agreement with the true undisturbed values.

IV. EXPERIMENTAL RESULTS

Two experiments have been carried out in a large anechoic room at the Technical University of Denmark. In the first experiment the source was a 3-mm aluminum plate with dimensions of 44×44 cm^2 mounted as one of the surfaces of a box of heavy fiberboard and excited by a loudspeaker inside the box. The sound pressure and the particle velocity were measured at 18×19 points in two planes of dimensions 42.5×45 cm^2 using a $\frac{1}{2}$-in. *p-u* intensity probe produced by Microflown. The transducer was calibrated as described in Ref. 24. The two measurement planes were 8 and 4.5 cm from the plate, and the measured data in the plane nearest the source were regarded as the true reference data. The equivalent sources were distributed in a plane 3 cm behind the plate. A Brüel & Kjær (B&K) "PULSE" analyzer (type 3560) was used for measuring the frequency responses between the pressure and particle velocity signals from the transducer and the signal generated by the PULSE analyzer (pseudorandom noise) for driving the source.

Figure 7 shows the results at 160 Hz. Parts (a)–(c) in the left column show the true pressure and the pressure predicted from measurements of pressure and predicted from measurements of particle velocity. It can be seen that the reconstruction based on the particle velocity is much better than the reconstruction based on the pressure. Parts (d)–(f) in the right column show the true particle velocity and the particle velocity predicted from measurements of pressure and predicted from measurements of particle velocity. It is apparent that the particle velocity reconstructed from the pressure is not very accurate, whereas the reconstruction based on measurement of particle velocity is far better. Similar results (not shown) have been obtained at other frequencies. In some cases (not shown) the pressure-to-pressure reconstruction was found to be slightly better than the velocity-to-pressure reconstruction, though, but velocity-to-velocity reconstruction was invariably found to be considerably better than the pressure-to-velocity reconstruction.

In the second experiment there were two sources. The primary source was a "coincident-source" loudspeaker unit produced by KEF mounted in a rigid plastic sphere with a diameter of 27 cm, and the disturbing source placed on the opposite side of the hologram plane was a B&K 4299 "volume velocity adaptor" (a 10-cm-long tube with an internal

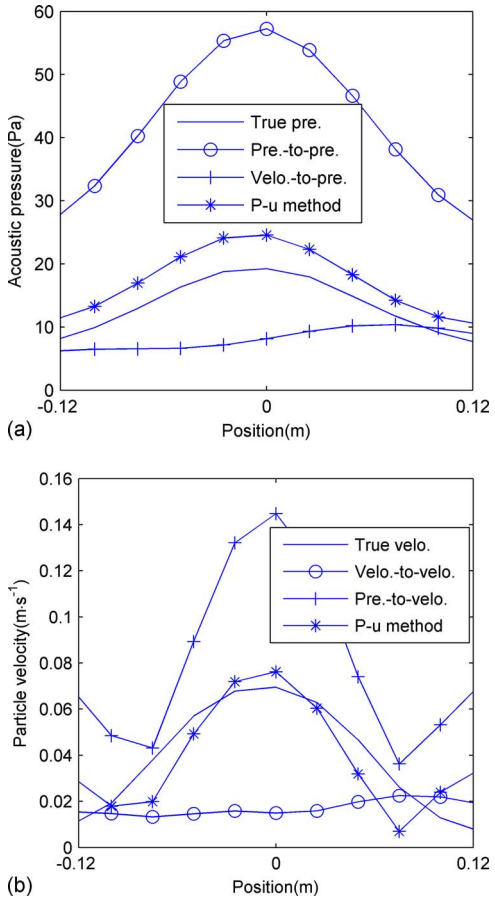

FIG. 8. (Color online) Sound field generated by a loudspeaker mounted in a sphere disturbed by sound from an experimental monopole at 528 Hz. True undisturbed pressure (a) and particle velocity (b) compared with predictions based on measurements of the pressure, the particle velocity, and both quantities using the *p-u* method.

diameter of 4 cm), mounted at the end of a long tube driven by loudspeaker (a B&K 4275 "OmniSource"). Because of its small opening this source is a good approximation to a monopole. The two sources were placed symmetrically with respect to the center of the measurement plane (of 25×25 cm^2) with a distance of 10 cm between them. The sound pressure and the particle velocity were measured at 11×11 points using the Microflown $\frac{1}{2}$-in. *p-u* intensity probe in the case when the two sources were operating together and the case when only the primary source was operating. The latter case provided the true reference data. In this case the hologram plane also served as the prediction plane, and the equivalent sources were placed 3 cm behind the front surface of the loudspeaker.

Figure 8 compares the true undisturbed pressure and particle velocity with predictions based on the pressure and based on the particle velocity, and predictions based on the *p-u* method at 528 Hz. The reconstructions based only on pressure or particle velocity give wrong results, but the reconstructions using the *p-u* method agree well with the true values. Similar results (not shown) have been found at other frequencies. However, because of resonances in the tube driven by the OmniSource the level of the disturbing sound varied strongly with the frequency, and at frequencies where this source was relatively weak compared with the primary

source reconstructions based on measurement of the particle velocity (not shown) were better than reconstructions based on the *p-u* method. The observation that the advantage of the *p-u* method vanishes when the disturbing sound is relatively weak has also been made with the statistically optimized version of NAH.[25] The explanation is that the *p-u* method relies critically on pressure- and particle velocity-based estimates being identical.

V. CONCLUSIONS

NAH based on the ESM and measurements with pressure-velocity transducers has been examined. Error sensitivity considerations demonstrate an advantage in using the normal component of the particle velocity rather than the pressure in the hologram plane as the input, and this advantage has been confirmed both by a simulation study and by experimental results. A variant of the method that combines pressure- and particle velocity-based estimates has also been examined and shown to perform well. This method makes it possible to distinguish between sounds coming from the two sides of the hologram plane.

ACKNOWLEDGMENTS

The authors would like to thank Microflown for lending a *p-u* sound intensity probe. This work was supported by the National Natural Science Foundation of China (Grant Nos. 50675056 and 10874037), the Fok Ying Tung Education Foundation (Grant No. 111058), and the Program for New Century Excellent Talents in University (Grant No. NCET-08-0767). Additionally, the China Scholarship Council is acknowledged for financial support.

[1]J. D. Maynard, E. G. Williams, and Y. Lee, "Nearfield acoustic holography: I. Theory of generalized holography and development of NAH," J. Acoust. Soc. Am. **78**, 1395–1413 (1985).
[2]W. A. Veronesi and J. D. Maynard, "Nearfield acoustic holography (NAH): II. Holographic reconstruction algorithms and computer implementation," J. Acoust. Soc. Am. **81**, 1307–1322 (1987).
[3]E. G. Williams, H. D. Dardy, and K. B. Washburn, "Generalized nearfield acoustical holography for cylindrical geometry: Theory and experiment," J. Acoust. Soc. Am. **81**, 389–407 (1987).
[4]M. R. Bai, "Application of BEM (boundary element method)-based acoustic holography to radiation analysis of sound sources with arbitrarily shaped geometries," J. Acoust. Soc. Am. **92**, 533–549 (1992).
[5]B.-K. Kim and J.-G. Ih, "On the reconstruction of the vibro-acoustic field over the surface enclosing an interior space using the boundary element method," J. Acoust. Soc. Am. **100**, 3003–3016 (1996).
[6]S.-C. Kang and J.-G. Ih, "Use of nonsingular boundary integral formulation for reducing errors due to near-field measurements in the boundary element method based near-field acoustic holography," J. Acoust. Soc. Am. **109**, 1320–1328 (2001).
[7]R. Steiner and J. Hald, "Near-field acoustical holography without the errors and limitations caused by the use of spatial DFT," Int. J. Acoust. Vib. **6**, 83–89 (2001).
[8]Y. T. Cho, J. S. Bolton, and J. Hald, "Source visualization by using statistically optimized nearfield acoustical holography in cylindrical coordinates," J. Acoust. Soc. Am. **118**, 2355–2364 (2005).
[9]Z. Wang and S. F. Wu, "Helmholtz equation-least-squares method for reconstructing the acoustic pressure field," J. Acoust. Soc. Am. **102**, 2020–2032 (1997).
[10]S. F. Wu and J. Yu, "Reconstructing interior acoustic pressure fields via Helmholtz equation least-squares method," J. Acoust. Soc. Am. **104**, 2054–2060 (1998).
[11]G. H. Koopman, L. Song, and J. Fahnline, "A method for computing acoustic fields based on the principle of wave superposition," J. Acoust. Soc. Am. **86**, 2433–2438 (1989).
[12]L. Song, G. H. Koopman, and J. Fahnline, "Numerical errors associated with the method of superposition for computing acoustic fields," J. Acoust. Soc. Am. **89**, 2625–2633 (1991).
[13]A. Sarkissian, "Extension of measurement surface in near-field acoustic holography," J. Acoust. Soc. Am. **115**, 1593–1596 (2004).
[14]A. Sarkissian, "Method of superposition applied to patch near-field acoustic holography," J. Acoust. Soc. Am. **118**, 671–678 (2005).
[15]C.-X. Bi, X.-Z. Chen, and J. Chen, "Nearfield acoustic holography based on the equivalent source method," Sci. China, Ser. E: Technol. Sci. **48**, 338–353 (2005).
[16]R. Jeans and I. C. Mathews, "The wave superposition method as a robust technique for computing acoustic fields," J. Acoust. Soc. Am. **92**, 1156–1166 (1992).
[17]F. Jacobsen and H.-E. de Bree, "A comparison of two different sound intensity measurement principles," J. Acoust. Soc. Am. **118**, 1510–1517 (2005).
[18]F. Jacobsen and Y. Liu, "Near field acoustic holography with particle velocity transducers," J. Acoust. Soc. Am. **118**, 3139–3144 (2005).
[19]F. Jacobsen and V. Jaud, "Statistically optimized near field acoustic holography using an array of pressure-velocity probe," J. Acoust. Soc. Am. **121**, 1550–1558 (2007).
[20]C.-X. Bi, X.-Z. Chen, and J. Chen, "Sound field separation technique based on equivalent source method and its application in nearfield acoustic holography," J. Acoust. Soc. Am. **123**, 1472–1478 (2008).
[21]C.-X. Bi and X.-Z. Chen, "Sound field separation technique based on equivalent source method using pressure-velocity measurements and its application in nearfield acoustic holography," Proceedings of Inter-Noise 2008, Shanghai, China.
[22]P. C. Hansen and D. P. O' Leary, "The use of the L-curve in the regularization of discrete ill-posed problems," SIAM J. Sci. Comput. (USA) **14**, 1487–1503 (1993).
[23]E. G. Williams, *Fourier Acoustics—Sound Radiation and Nearfield Acoustical Holography* (Academic Press, San Diego, 1999).
[24]F. Jacobsen and V. Jaud, "A note on the calibration of pressure-velocity sound intensity probes," J. Acoust. Soc. Am. **120**, 830–837 (2006).
[25]F. Jacobsen, X. Chen, and V. Jaud, "A comparison of statistically optimized near field acoustic holography using single layer pressure-velocity measurements and using double layer pressure measurements," J. Acoust. Soc. Am. **123**, 1842–1845 (2008).